

THE OFFICIAL MAGAZINE OF THE OCEANOGRAPHY SOCIETY

Oceanography

CITATION

Yang, K.-C., J. Wang, C.M. Lee, B. Ma, R.-C. Lien, S. Jan, Y.J. Yang, and M.-H. Chang.
2015. Two mechanisms cause dual velocity maxima in the Kuroshio east of Taiwan.
Oceanography 28(4):64–73, <http://dx.doi.org/10.5670/oceanog.2015.82>.

DOI

<http://dx.doi.org/10.5670/oceanog.2015.82>

COPYRIGHT

This article has been published in *Oceanography*, Volume 28, Number 4, a quarterly journal of The Oceanography Society. Copyright 2015 by The Oceanography Society. All rights reserved.

USAGE

Permission is granted to copy this article for use in teaching and research. Republication, systematic reproduction, or collective redistribution of any portion of this article by photocopy machine, reposting, or other means is permitted only with the approval of The Oceanography Society. Send all correspondence to: info@tos.org or The Oceanography Society, PO Box 1931, Rockville, MD 20849-1931, USA.

Seaglider deployment in Luzon Strait.
Photo credit: Kai-Chieh Yang

Two Mechanisms Cause Dual Velocity Maxima in the Kuroshio East of Taiwan

By Kai-Chieh Yang, Joe Wang,
Craig M. Lee, Barry Ma,
Ren-Chieh Lien, Sen Jan,
Yiing Jang Yang, and
Ming-Huei Chang

ABSTRACT. We examine velocity structure and variability across the Kuroshio east of Luzon and Taiwan using two years of Seaglider observations. The Kuroshio exhibits a single velocity maximum south of Luzon Strait, strengthened downstream. It is occasionally accompanied by a second velocity maximum, and the two together form a dual-core structure east of Taiwan. Two possible mechanisms are responsible for the dual-core phenomenon. One is attributed to intrusion of the Kuroshio into the South China Sea through Luzon Strait, which occurs normally during persistent northeasterlies in winter. The streamline diffuence across the strait during the Kuroshio's westward intrusions and subsequent shaping of the boundary current through interaction with a quasi-permanent anticyclonic recirculation east of Taiwan favors the appearance of the offshore velocity maximum. The other possible mechanism is related to the dissipation of westward-propagating mesoscale anticyclonic eddies. As the impinging eddy deforms and is eventually dissipated along the Kuroshio's eastern flank, the northward flow contiguous to the western half of this eddy is enhanced, causing an offshore core downstream. Glider-observed θ - S properties in the dual cores indicate different water masses are mixing, consistent with two different mechanisms causing the dual cores.

INTRODUCTION

The Kuroshio, the western boundary current (WBC) of the North Pacific, originates at the bifurcation of the North Equatorial Current (NEC) as it encounters the Philippine coast. Here, the NEC partitions into the north-flowing Kuroshio Current and the south-flowing Mindanao Current (Nitani, 1972; Figure 1). The Kuroshio flows northward along the east coast of Luzon across, and sometimes into, the 350 km wide Luzon Strait, and continues its journey northward along the east coast of Taiwan, into the East China Sea and along the coast of Japan. Although it is difficult to discern near the bifurcation region, the Kuroshio strengthens and becomes more distinct as it transits between Luzon and Taiwan, a region Nitani (1972) defines as the “beginning of the Kuroshio.”

The WBC systems of the North Pacific (Kuroshio) and North Atlantic share many characteristics, including latitudinal range and the presence of straits connecting to marginal seas along their pathways (Luzon Strait and the South China Sea [SCS] for the Kuroshio and Yucatán Channel/Straits of Florida and the Gulf of Mexico for the North Atlantic WBC system. Strictly speaking, the North Atlantic

WBC system downstream of the Straits of Florida is referred to as the Gulf Stream.) Both play important roles in transporting heat, salt, and momentum in the ocean from the tropics to mid-latitudes. Differences in pathway bathymetry, coastline geometry, atmospheric forcing, and other parameters drive differences between the two WBCs. For example, the North Atlantic WBC often penetrates the Yucatán Channel and flows into the Gulf of Mexico to form the anticyclonic Loop Current, which can pinch off to produce anticyclonic eddies. In contrast, the Kuroshio rarely forms an anticyclonic loop current in the northern SCS (Chern et al., 2010). While the Florida Current/Gulf Stream entrains little water from the Gulf of Mexico (Pickard and Emery, 1993), when the Kuroshio intrudes Luzon Strait, it entrains waters from the SCS and carries this modified water mass within its western flank as it flows northward east of Taiwan (Chern and Wang, 1998).

Recent observations collected by two collaborating programs, Observations of the Kuroshio Transports and their Variability (OKTV; Jan et al., 2015) and Origins of the Kuroshio and Mindanao Currents (OKMC; e.g., Rudnick et al., 2011; Lien et al., 2014), reveal variability

of the Kuroshio core position and mass transport east of Taiwan that is of comparable magnitude to its climatological mean (Jan et al., 2015). In this region, historical shipboard acoustic Doppler current profiler (Sb-ADCP) data (Liang et al., 2003) and recent, repeated, ship-based zonal sections at $\sim 23^{\circ}45'N$ (Jan et al., 2015) show that the Kuroshio sometimes exhibits two distinct velocity maxima (referred to as “dual-core” hereafter). The potential impact of this dual-core structure on the Kuroshio's mass, heat, and salt transport motivates this attempt to understand the dynamics that drive the observed structure.

Chern and Wang (1998) first reported the dual-core structure from an analysis of a hydrographic section extending east of Taiwan at $23^{\circ}40'N$ taken from August 28 to September 10, 1994. Geostrophic velocities (referenced to a 1,000 m level of no motion) revealed two distinct velocity maxima that were attributed to upstream splitting of the Kuroshio by the ridge east of Luzon Strait (the Luzon volcanic arc). Liang et al. (2003) used archived Sb-ADCP data (1991–2000) to produce composite sections at $22^{\circ}N$ and $23^{\circ}N$ that also revealed a dual-core structure confined to the upper 300 m, with the inshore velocity maxima being generally stronger and more surface intensified than the offshore maxima. They attributed this structure to a combination of Kuroshio separation by local topography near Lanyu Island and splitting in Luzon Strait. The composite sections of Liang et al. (2003) also suggest that the two velocity cores merge in the vicinity of $23^{\circ}45'N$, before the Kuroshio passes over I-Lan Ridge east of Taiwan. Hsin et al. (2008) report similar dual-core structures at $22^{\circ}30'N$ in numerical simulations, speculating that the inshore core forms from the Kuroshio loop current near the southern tip of Taiwan, and the offshore core originates as an extension of northward flow

east of Batan Island. More recently, Jan et al. (2015) report dual-core structures observed in three of nine ship-based surveys conducted between September 2012 and September 2014 east of Taiwan at 23°45'N. These data suggest that the dual-core structure can remain distinct even north of 23°N, contrary to the more southern merger described in Liang et al. (2003) and Hsin et al. (2008).

Our study builds on previous investigations by quantifying spatial and temporal variability of dual-core structures and investigating possible formation mechanisms. We begin with an overview of mean current patterns in the vicinity of Luzon Strait and quantification of dual-core structures east of Taiwan using observations collected by autonomous underwater gliders and satellite altimetry.

Variations in hydrographic properties within dual-core structures provide information about their origins. We then examine possible generation mechanisms for dual-core structures, and provide some conclusions from our study.

OBSERVATIONS

This study uses profiles of temperature and salinity across the Kuroshio collected by long-endurance autonomous Seagliders. The Seaglider is a 50 kg, 2 m long, buoyancy-driven autonomous underwater vehicle designed to glide from the ocean surface to as deep as 1,000 m while measuring water properties that include temperature, salinity, pressure, and dissolved oxygen concentration, as well as bio-optical variables (Eriksen et al., 2001). Seagliders steer

through the water by controlling attitude (pitch and roll) and can thus navigate between waypoints to execute survey patterns. Although Seagliders move through the water slowly, at speeds of roughly 20 km per day, they can successfully navigate across strong currents such as the Kuroshio. When at the sea surface between dives, Seagliders acquire position information through GPS and download new commands and upload data via Iridium satellite phones. The vehicles navigate by dead reckoning when below the surface. Depth-averaged water velocity (averaged over the vertical range of a dive; v_{dac}) can be calculated by taking the difference between the glider's anticipated displacement, which is calculated using a hydrodynamic model that estimates flight path based on glider attitude and buoyancy, and its actual displacement (position at the end of the dive relative to position at the beginning).

As a component of OKMC, a total of 14 Seaglider missions, conducted between June 2011 and July 2013, provide over 10,000 profiles along two triangular survey patterns east of Luzon Strait (Figure 1a). The three sides of the triangle are designated N1, N2, and N3 east of Taiwan and S1, S2, and S3 northeast of Luzon Island.

Current velocities from historical Sb-ADCP, contemporaneous estimates of geostrophic surface currents derived from Archiving, Validation and Interpretation of Satellite Oceanographic data (AVISO) sea surface height (SSH), and v_{dac} (0–1,000 m) estimated from Seagliders were used to assess the angle at which Seaglider-targeted sections traversed the Kuroshio. Comparisons of average Seaglider section orientations (expressed as the direction perpendicular to Seaglider sections) with average Kuroshio orientations (Table 1) were calculated from (1) historical Sb-ADCP data from the Taiwan Ocean Data Bank, and (2) AVISO-derived surface geostrophic currents for the time period of each section. The strongest v_{dac} show good agreement along Seaglider sections S2 and N1,

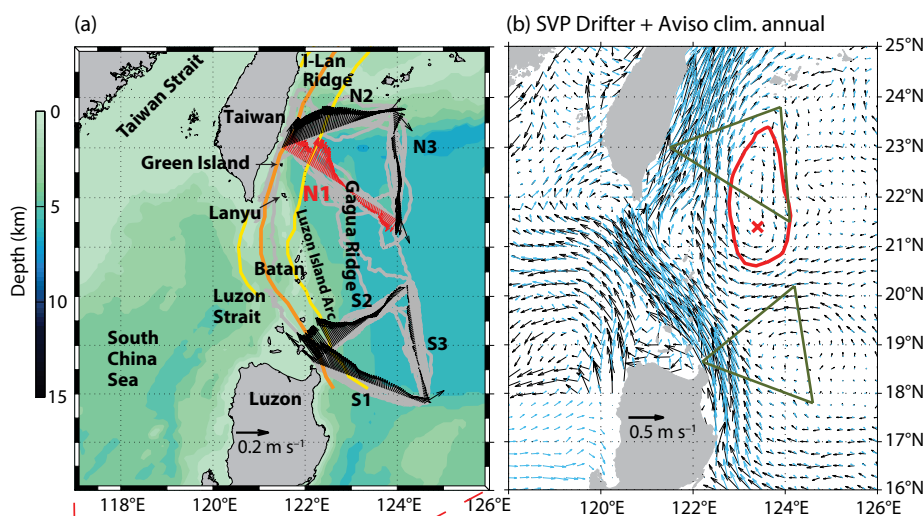


FIGURE 1. (a) Bathymetry chart, Seaglider tracks (gray lines), and time-averaged depth-averaged current from multiple Seaglider surveys along the same section taken between 2011 and 2013 in the vicinity of Luzon Strait. Section N1, the focus in this study, is highlighted in red. The orange line indicates mean axis position of the Kuroshio defined by the maximum velocity axis at 15 m depth from surface drifter trajectories (available at <http://www.coriolis.eu.org>). The yellow line indicates mean boundaries of the Kuroshio defined by the 0.2 m s⁻¹ isotach at 30 m depth from the historical ADCP data set. (b) Climatological current velocity from surface drifters (black arrows) and geostrophic velocity inferred from AVISO sea surface height (SSH; blue arrows) from 1993 to 2013. The green solid lines indicate Seaglider-targeted transects. The red "x" and red enclosed line mark the mean positions of the center and the area of recirculation, defined by local SSH maximum and the largest enclosed contour of streamlines inferred from AVISO geostrophic current east of Taiwan, respectively. The current velocity reference scale is labeled in the lower part of each panel.

suggesting that sections were well oriented at these locations to provide nearly perpendicular crossings of the boundary current. Sections S1 and N2 crossed the Kuroshio at more oblique angles. Individual glider trajectories sometimes deflect from the specified track line (off-track displacements varied between 0 and 110 km), though in 90% of cases the displacements are modest (<35 km). Hydrographic profiles from each dive, averaged into 5 m vertical bins, were thus projected onto the straight target track lines to reduce distortions that could arise from oblique sampling of the current. Processed data were then interpolated to a 2 km horizontal grid and 48 h low-pass filtered (analogous to a 30 km spatial filter given typical transit speeds across the Kuroshio) to exclude high-frequency fluctuations in the data. The resulting temperature and salinity sections across the Kuroshio were combined with collocated estimates of v_{dac} to quantify the structure and variability of the Kuroshio east of Taiwan.

Based on previous studies and observations, this study defines two characteristics of dual-core structures. First, the positions of dual velocity cores must be within the Kuroshio, and second, speeds must exceed 0.4 m s^{-1} . Events driven by active impinging anticyclonic eddies are

excluded by identifying eddy-Kuroshio interactions using AVISO SSH anomaly (SSHA) and corresponding absolute geostrophic surface velocities. We also exclude events where the distance between two cores is shorter than the Nyquist sampling length scale (approximately 12 km for Seaglider surveys).

MEAN FLOW PATTERN

Time-averaged v_{dac} (averaged over the two-year period of Seaglider sampling; Figure 1a) are relatively strong adjacent to the coast in the N1, N2, S1, and S2 sections, generally within but slightly broader than the climatological width of the Kuroshio (defined by meridional velocity $v \geq 0.2 \text{ m s}^{-1}$ at 30 m depth from the historical Sb-ADCP data set; Jan et al., 2015). The two-year mean shows a single Kuroshio velocity maximum south of Luzon Strait (S1 and S2), but indicates likely dual maxima at N1, with the inshore core west of 122°E and the offshore core situated between Green Island and the Gagua Ridge. Note that this dual-core structure might include an artifact of averaging northward current at depth, which is not the focus of this paper. The standard deviation of v_{dac} computed from nine surveys along N1 is $\sim 0.1 \text{ m s}^{-1}$ (not shown). Further to the north (N2), the Kuroshio appears as a single, broad flow.

Southward mean currents dominate along N1 east of Gagua Ridge and over the southern half of N3 (Figure 1a). Though fluctuations of v_{dac} are of the same order of magnitude as the mean current, observed northward mean currents along the western half of N1, reversing to southward flow further offshore, are consistent with a possible anticyclonic recirculation east of Taiwan and Luzon Strait. Composite velocity maps derived from surface drifters and climatological geostrophic velocity inferred from AVISO SSH for the period 1993–2013 (Figure 1b) show similar anticyclonic recirculation, indicative of a persistent feature. By tracking local SSH maxima in monthly climatological maps, we obtained estimates of the recirculation center position for each month of the year (colored dots in Figure 2a). The recirculation centers at approximately $21^\circ 36'\text{N}$, $123^\circ 24'\text{E}$ in winter (December–February), moves southwestward to $21^\circ 24'\text{N}$, $123^\circ 24'\text{E}$ in spring (March–May), reaches its southernmost position at approximately $21^\circ 06'\text{N}$, $123^\circ 36'\text{E}$ in summer (June–August), and shifts northward to $21^\circ 12'\text{N}$, $123^\circ 36'\text{E}$ in fall (September–November). The center position normally sits east of the meridional Gagua Ridge (Figure 2a–c). SSH at the recirculation center changes seasonally, with the highest values occurring in summer.

TABLE 1. (1) Seaglider section orientation compared to Kuroshio orientation derived from: (2) historical Sb-ADCP data ($v_{Sb-ADCP}$) from the Taiwan Ocean Data Bank, (3) AVISO-derived surface geostrophic currents (v_{AVISO}) for the time period of each section, and (4) the strongest depth-averaged (0–1,000 m) velocities (v_{dac}) estimated from Seaglider data.

	S2	N1
(1) Seaglider section	321°	32°
(2) $v_{Sb-ADCP}$	322°	31°
(3) v_{AVISO}	$328^\circ \pm 4^\circ$	$25^\circ \pm 8^\circ$
(4) v_{dac}	$328^\circ \pm 8^\circ$	$32^\circ \pm 27^\circ$

NOTE: Orientation is given in degrees clockwise from true north.

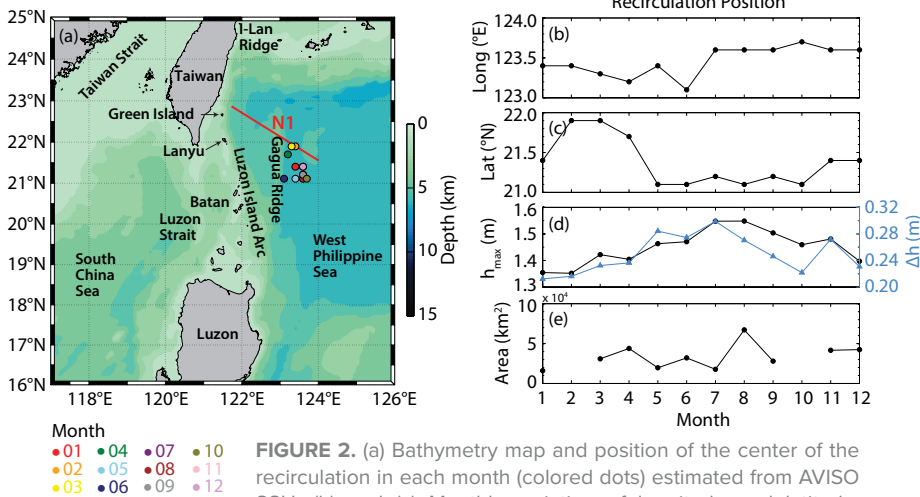


FIGURE 2. (a) Bathymetry map and position of the center of the recirculation in each month (colored dots) estimated from AVISO SSH. (b) and (c) Monthly variation of longitude and latitude, respectively, at the center of recirculation. (d) Monthly variation of SSH at the recirculation center (black) and the difference in SSH between the recirculation center and the Kuroshio axis southeast of Taiwan (blue). (e) Monthly variation of the recirculation area.

The difference in SSH between the center of the recirculation and the Kuroshio axis is larger in summer than in winter (Figure 2d), and the size of the recirculation, defined as the largest enclosed contours of streamlines inferred from AVISO geostrophic current east of Taiwan, varies mildly with time, greater in summer than in the other seasons (Figure 2e).

GEOSTROPHIC CURRENT AT SECTION N1

Glider-based sampling allows computation of absolute geostrophic velocity normal to the direction of travel. Relative geostrophic velocity (v_{rel}) referenced to an arbitrary depth (here chosen as 1,000 m) can be estimated using the thermal wind relation

$$\frac{\partial v_{rel}}{\partial z} = -\frac{g}{\rho_0 f} \frac{\partial \rho}{\partial x},$$

where x and z are the along-section and vertical axes, ρ_0 ($= 1,025 \text{ kg m}^{-3}$) is a

reference density, ρ is density calculated from temperature, conductivity, and pressure measured by Seaglider, f is the local Coriolis parameter, and g ($= 9.81 \text{ m s}^{-2}$) is gravitational acceleration. This can be combined with depth average velocity (v_{dac}) to yield absolute geostrophic velocity (v_{abs}):

$$v_{abs}(x, z) = \overline{v_{rel}(x, z) + v_{dac}(x) - v_{rel}(x, z)},$$

where the overbar indicates a depth average (over the same range as v_{dac}). The v_{abs} at N1 reveals the Kuroshio core centered at $121^\circ 36'E \pm 4.8'$, near the west end of N1, with a mean maximum velocity of 1 m s^{-1} and a standard deviation of 0.24 m s^{-1} (Figure 3a–i). Note that the target section N1 is nearly perpendicular to the Kuroshio (Table 1), so the underestimates/overestimates due to oblique sampling are assumed insignificant. Even though Seaglider surveys miss a portion of the Kuroshio at its

western/shoreward edge due to the territorial water restriction, our results are comparable to historical Sb-ADCP current velocity at 23°N , which shows the Kuroshio centered at $121^\circ 30'E$ with a mean maximum velocity of $\sim 1 \text{ m s}^{-1}$ and a standard deviation of $\sim 0.4 \text{ m s}^{-1}$. The core shifts shoreward during the northeast monsoon (Figure 3j). Taking the $v_{abs} = 0.2 \text{ m s}^{-1}$ isotach as the entire Kuroshio boundary, the Kuroshio thickness ranges between 200 m and 800 m across the nine surveys. Surveys 1, 4, and 5 show signs of impact from impinging mesoscale anticyclonic eddies (Figure 3a,d,e) identified from contemporaneous AVISO SSHA (not shown). The collection includes three dual-core events in Survey 2 (November 27–December 13, 2011, Figure 3b), Survey 3 (January 2–20, 2012, Figure 3c) and Survey 8 (January 2–February 4, 2013, Figure 3h), all during the northeast monsoon. Survey 2 captured the strongest v_{abs} among these events. Separation distance between inshore and offshore velocity cores varies between 34 km and 75 km. The positions of the offshore velocity core during Surveys 2, 3, and 8 are located at $121^\circ 56'E$, $122^\circ 22'E$, and $122^\circ 05'E$, respectively (Figure 3j). The maximum velocities of the respective inshore/offshore velocity cores for Surveys 2, 3, and 8 are $1.3/0.8$, $0.7/0.6$ and $1.1/0.7 \text{ m s}^{-1}$, respectively.

WATER MASSES ASSOCIATED WITH THE DUAL VELOCITY MAXIMA

Water mass analysis (for temperature and salinity) can help identify the sources of waters observed in the Kuroshio cores. Characteristics of N1 θ – S (Surveys 2, 3, and 8; Figure 4a–c) for waters within the Kuroshio dual cores (defined as $v_{abs} > 0.4 \text{ m s}^{-1}$ to isolate two cores) provide a way to identify the source of waters found within the current. Average θ – S curves for SCS, West Philippine Sea (WPS), and Kuroshio-origin (labeled as NEC) waters (Mensah et al., 2014) provide reference points for possible sources. Seaglider data from transect N1 reveal

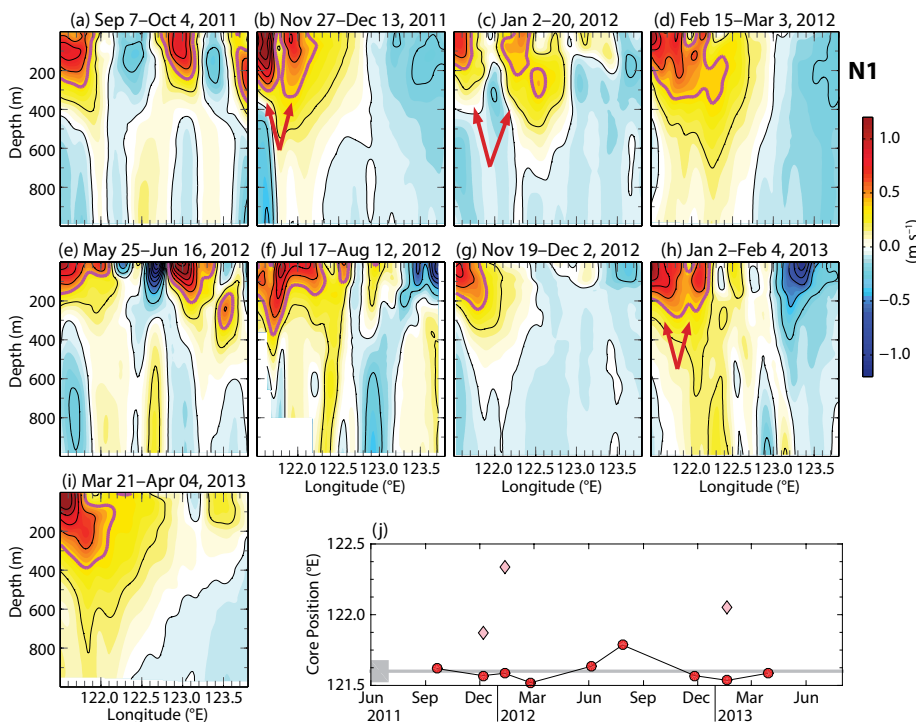


FIGURE 3. (a–i) Cross sections of absolute geostrophic velocity (v_{abs}) derived from Seaglider-measured hydrography data and v_{dac} during Surveys 1–9 along section N1. Velocity contours are plotted with an interval of 0.2 m s^{-1} in black and of 0.4 m s^{-1} in magenta. Red arrows point to the dual-core events during Survey 2, 3, and 8. (j) The positions of the Kuroshio velocity maximum core (filled red circle) from all surveys, and the offshore velocity core (filled pink diamond) from Surveys 2, 3, and 8. The gray line and shaded area represent mean and standard deviation of the Kuroshio main axis position.

a salinity maximum of 34.8 between $23.5 < \sigma_\theta < 24.5 \text{ kg m}^{-3}$ ($\sim 200 \text{ m}$ depth or $\sim 18^\circ\text{C}$ isotherm) associated with North Pacific Tropical Water (NPTW) and a salinity minimum of 34.3 between $26.5 < \sigma_\theta < 27 \text{ kg m}^{-3}$ ($\sim 600 \text{ m}$ depth or $\sim 7^\circ\text{C}$ isotherm) associated with North Pacific Intermediate Water (NPIW). Direct atmospheric forcing (net surface heat flux and wind-driven mixing) primarily impact the surface mixed layer, typically shallower than 100 m in this region. Thus, we ignore the impacts of direct atmospheric forcing on the salinity extrema (NPTW and NPIW).

When the two velocity cores are closest together (Survey 2), SCS Tropical Water (SCSTW) dominates the inshore core, manifesting as a relatively weak 34.6 salinity maximum at the western end of the section, and presumably mixes with WPS water further to the east. Waters within the offshore velocity core are a mixture of WPS and NEC tropical waters. Survey 3 also exhibits cores with distinct θ - S properties. The inshore core is primarily SCSTW while the offshore core is close to WPS Tropical Water (WPSTW). The existence of SCS water on the western (inshore) flank of the Kuroshio is consistent with entrainment during the Kuroshio's passage through Luzon Strait (Chern and Wang, 1998; Chen, 2005; Mensah et al., 2014). However, the two cores observed during Survey 8 differ from this pattern, with both inshore and offshore cores composed primarily of WPS water.

MECHANISMS FOR THE DUAL VELOCITY MAXIMA

AVISO SSH maps reveal differences in circulation underlying the two classes of dual-core events (Figure 4d–f). During Surveys 2 and 3, the Kuroshio intruded Luzon Strait to form loop currents in the northern SCS, likely entraining SCS water and carrying it northward along the east coast of Taiwan, consistent with the existence of SCSTW in the inshore core mentioned in the previous section. The position and strength of the quasi-permanent

anticyclonic recirculation southeast of Taiwan likely impacts the location and strength of the offshore core. Survey 8 lies within a different circulation pattern, where the Kuroshio crosses Luzon Strait without intruding the SCS. The two cores east of Taiwan thus show little SCS influence, consistent with Seaglider-observed θ - S properties during Survey 8. A narrow, meridionally elongated anticyclonic circulation pattern is located east of Luzon Strait, contributing to the observed northward flow at N1.

Two mechanisms may contribute to the formation of the dual-core structure: (1) entrainment during the Kuroshio's westward intrusions into the SCS and subsequent shaping of the boundary current through interaction with the quasi-permanent anticyclonic recirculation east of Taiwan, and (2) interactions between the Kuroshio and westward-propagating anticyclonic eddies east of Luzon Island. To quantify how the first process might contribute to the dual-core structure, relative vorticity, calculated from AVISO

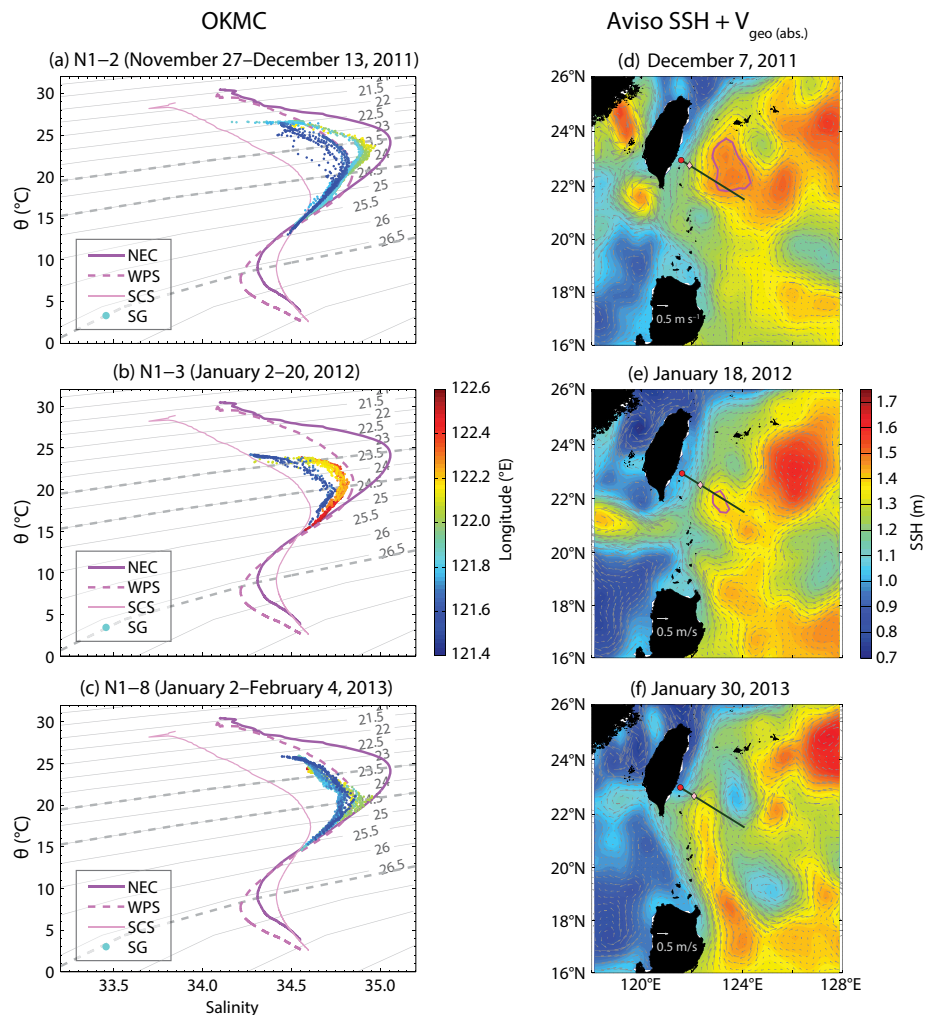


FIGURE 4. (a–c) θ - S diagrams within dual velocity maxima (only for $v_{\text{abs}} > 0.4 \text{ m s}^{-1}$) using Seaglider (SG) data acquired along section N1 during Surveys 2, 3, and 8, colored by longitudes associated with the sampling position. The thin solid, dashed, and thick solid purple lines are the averaged θ - S curves for South China Sea (SCS) water, West Philippines Sea (WPS) water, and North Equatorial Current (NEC) waters east of Luzon Island, respectively. Gray dashed lines are the ranges of the salinity maximum of the Kuroshio water defined by Mensah et al. (2014) and the base of the Kuroshio main velocity core from Lien et al. (2014). (d–f) AVISO SSH (color shading) and corresponding geostrophic current during each of Surveys 2, 3, and 8. The green solid line indicates the Seaglider transect along N1. The magenta enclosed line marks the area of the anticyclonic recirculation southeast of Taiwan. The filled red circle and pink diamond represent positions of the inshore and offshore velocity cores, respectively.

SSH, was used to estimate the position of the Kuroshio's velocity maximum, taken as the location where relative vorticity crosses zero. The positions of the SSH-based Kuroshio velocity maxima are located 10–35 km offshore from the positions of maxima identified from Sb-ADCP surveys (Liang et al., 2003; Jan et al., 2015). These differences might be artifacts of the limited temporal and spatial resolution (~150 km; Ducet et al., 2000) provided by mapped satellite

altimetry products, which would cause errors in studies of currents with a narrow width scale. Lien et al. (2015) show that the Kuroshio surface current east of Luzon derived from AVISO is spatially heavily smoothed and its maximum current speed is underestimated by nearly 50% compared with direct observations from moorings, Seagliders, and drifters.

Monthly maps of Kuroshio position reveal a greater tendency for it to intrude the SCS through Luzon Strait

during winter (Figure 5a–d,k,l, magenta dots). The Kuroshio's path in the vicinity of Luzon Strait is thought to be modulated by the seasonally reversing East Asian monsoon, with strong northeasterlies in winter (northeast monsoon, October–April), relatively weaker southwesterlies in summer (southwest monsoon, May–September), and transition in April–May and September–October (Farris and Wimbush, 1996; Metzger and Hurlburt, 2001). In addition, a separated northward branch of the Kuroshio passes east of Batan Island to the southeast of Taiwan more frequently in winter than in summer. This northward flow has speeds of 0.2–0.3 m s^{−1} and is relatively stable compared with the Kuroshio main stream, which has stronger seasonal speed variability.

Jets and velocity maxima form in response to the strengthening of the lateral density gradients, which requires a confluence of streamlines (Cushman-Roisin, 1994). This process may be quantified by deformation rate. Deformation changes the horizontal density gradient (if any) across the flow by advection. For a quasi-geostrophic flow, vertical shear of horizontal velocity responds to changes in the lateral density gradient through the thermal wind relation. Confluent flows sharpen the horizontal density gradient and thus accelerate the flow, assuming no changes in the barotropic component. For example, assume a purely northward flowing Kuroshio. The zonal stretching deformation rate at the sea surface (D_x) is defined as

$$D_x = \frac{\partial u_g}{\partial x} - \frac{\partial v_g}{\partial y} = 2 \frac{\partial u_g}{\partial x}, \quad (1)$$

assuming a horizontally nondivergent geostrophic current, where u_g and v_g are surface zonal and meridional geostrophic velocities inferred from AVISO SSH. Positive D_x indicates diffuence of streamlines, weaker zonal density gradients, and therefore weaker northward currents. Negative D_x indicates confluence of streamlines, stronger zonal density gradients, and therefore stronger

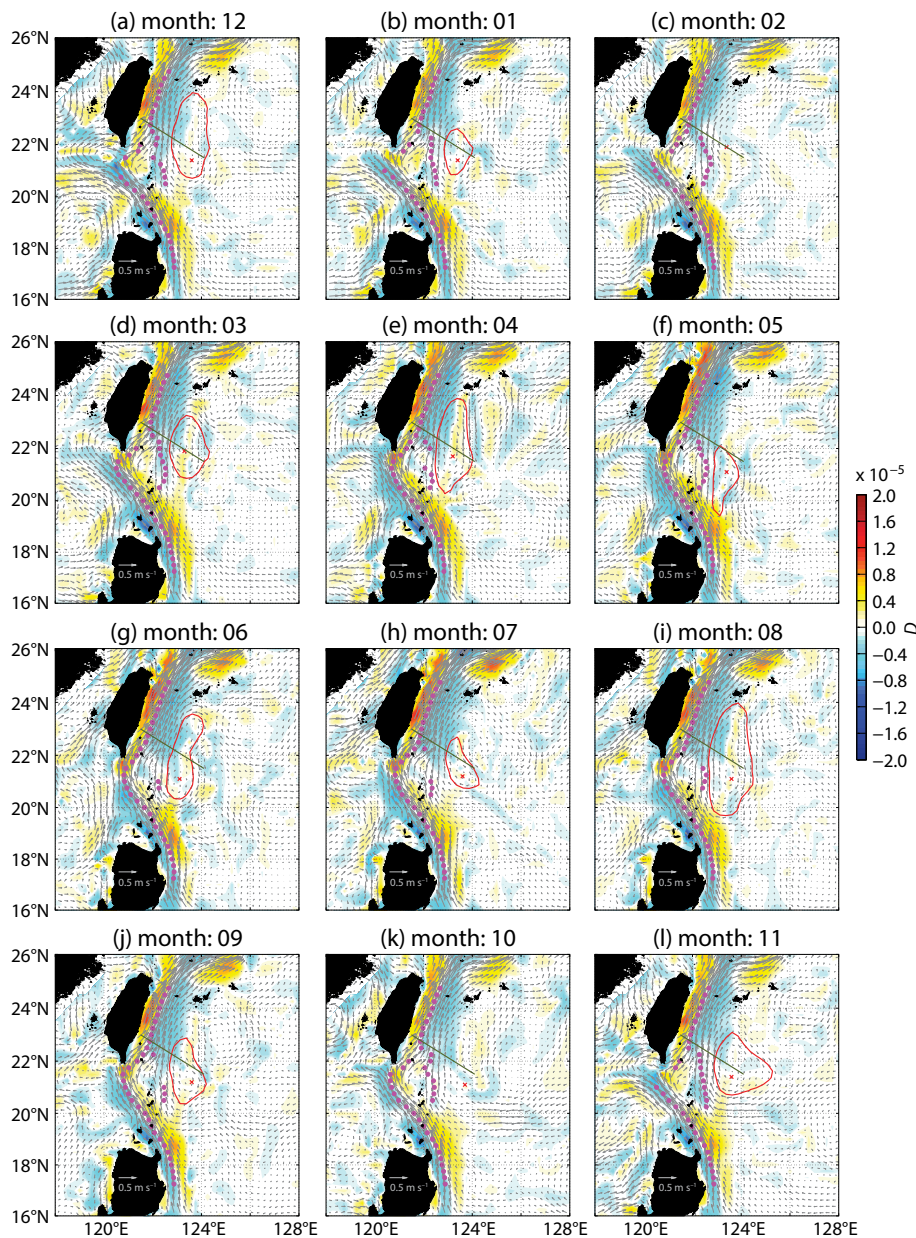


FIGURE 5. Monthly climatological deformation rates (D) estimated from AVISO SSH. Magenta dots represent positions of the Kuroshio main axis and the core of the northward flow east of Luzon Strait. The green solid line indicates the Seaglider transect along N1. A red “x” and a red enclosed line mark the positions of the center and the area of recirculation, respectively.

northward currents.

The deformation rate (D) of any general streamline can be defined on its natural coordinates (n - s), in which n is perpendicular to and s is along the streamline direction (Saucier, 1955), as

$$D = V_g \frac{\partial \varphi}{\partial n} - \frac{\partial V_g}{\partial s} = -2 \frac{\partial V_g}{\partial s} \\ = 2 \left(\frac{\partial u_g}{\partial x} \cos 2\varphi + \frac{1}{2} \left(\frac{\partial v_g}{\partial x} + \frac{\partial u_g}{\partial y} \right) \sin 2\varphi \right) \\ = 2 \underbrace{\frac{g}{f} \frac{\partial^2 h}{\partial x \partial y} \cos 2\varphi}_{\text{compression}} \\ + \underbrace{\frac{g}{f} \left[\left(\frac{\partial^2}{\partial x^2} - \frac{\partial^2}{\partial y^2} \right) h \right] \sin 2\varphi}_{\text{stretching}}. \quad (2)$$

Here, V_g is geostrophic velocity along the streamline, φ is flow direction in degrees of azimuth clockwise from true north, and h is sea surface height. The first term on the right-hand side of the equation represents flow compression, and the second term represents stretching along the flow. For a northward streamline, $\varphi = 0$ and D becomes identical to D_x , as in Equation 1. Positive/negative D represents lateral diffiuse/confluence of streamlines with accompanying deceleration/acceleration of the flow.

Maps of monthly mean D show a pattern of confluence/diffiuse along the west/east flank of the Kuroshio when it deflects toward the west from southern Luzon Strait (Figure 5). The spatial distribution of D reverses northward along the Kuroshio east of Taiwan, which suggests acceleration of the current. The Kuroshio usually curves more westward when flowing across Luzon Strait during the northeast monsoon (Centurioni et al., 2004; Yuan et al., 2006). This westward intrusion of the Kuroshio causes streamline diffiuse at $\sim 21^\circ 30'N$, between Batan Island and Lanyu Island, weakening the northward current in Luzon Strait (Figure 5a–d,k,l). The other northward branch of the Kuroshio, which passes east of Luzon

Strait to contribute to the offshore core east of Taiwan, remains unchanged and thus becomes relatively distinct (the clear axis of this northward flow east of Batan Island in Figure 5a–d,k,l). Together with the northward shift of anticyclonic recirculation during the northeast monsoon, this westward intrusion of the Kuroshio causes the region of confluent streamlines east of Taiwan to move downstream. During the southwest monsoon, the recirculation migrates southward (Figures 2c and 5g–j) and the Kuroshio strengthens, producing streamline confluence between Batan Island and Lanyu Island (Figure 5g–j).

Figure 6 illustrates conditions during the two phases of the monsoon. The Kuroshio's path and the position of the recirculation control the confluence/diffiuse of streamlines in the vicinity of Luzon Strait, especially east of Batan and Lanyu Islands where the offshore branch of the Kuroshio is located (dashed line in Figure 6). The joint effect of the Kuroshio and the recirculation further determine the appearance of dual-core structures downstream. For example, the region of streamline confluence among the Kuroshio main path, its offshore branch, and the recirculation retreats downstream (east of Taiwan) during the northeast monsoon due to the Kuroshio intrusion and northward shift of the recirculation, while during the southwest monsoon,

the streamline confluence occurs further south between Batan Island and Lanyu. The available sections suggest that dual-core structures are more prevalent in winter than in summer, with most observations showing these events occurring during the northeast monsoon (Jan et al., 2015). Chern and Wang (1998) document an exception during summer (August 28–September 10, 1994). A typhoon passed through Luzon Strait a few days before their ship-based survey, resulting in a westward shift of the Kuroshio in Luzon Strait.

Interactions between the Kuroshio and anticyclonic eddies provide another mechanism for producing dual-core structures that is not subject to the seasonality that modulates the intrusion/recirculation mechanism. Figure 7 is a sequence of AVISO SSHA that shows surface geostrophic velocity maps illustrating the evolution of an anticyclonic eddy impinging on the Kuroshio. An anticyclone is initially identified at approximately $15^\circ N$, $130^\circ E$ in early October 2012 (documented in Lien et al., 2014) propagating westward with the NEC. It impinges on the Kuroshio at a mean speed of 0.2 m s^{-1} in December 2012, at which point its center appears to stall offshore of Luzon (Figure 7a–c). The eddy deforms and elongates to the north during its interaction with the Kuroshio (Figure 7d–h), disappearing in SSHA

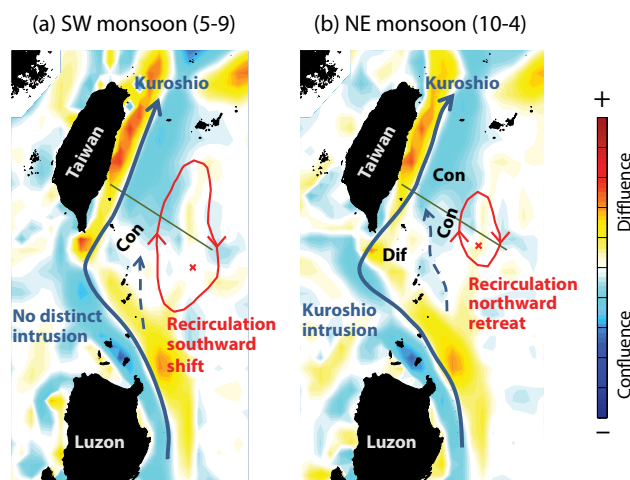


FIGURE 6. Schematics showing the appearance of dual velocity maxima as a result of the joint effect of the Kuroshio's westward intrusion in Luzon Strait and the recirculation east of Taiwan during (a) southwest and (b) northeast monsoon periods. Color shading indicates corresponding D (deformation rate of any general streamline) estimated from AVISO SSH. Abbreviation "Dif"/"Con" represents the diffiuse/confluence of streamlines.

Blue solid and dashed lines represent the Kuroshio main axis and its offshore branch. A red "x" and an enclosed line mark the positions of the center and the area of recirculation, respectively.

around January 23, 2013 (Figure 7i). A meridional, narrow high-pressure patch remained after the eddy dissipated (Figure 7i,j). Northward surface geostrophic currents spatially averaged over the region east of Luzon Strait ($20^{\circ}45'N$ – $21^{\circ}5'N$, $122^{\circ}E$ – $122^{\circ}24'E$) from AVISO (Figure 7k) show significant acceleration east of the strait during the time when the eddy is dissipating (January 9–30, 2013), reaching a maximum of 0.44 m s^{-1} on January 30, when the dual-core event during Survey 8 was observed. As suggested by Kuo and Chern

(2011), during eddy-WBC interaction, northward flow is enhanced along the western rim of the eddy, which increases horizontal velocity shear and friction along the western boundary, leading to dissipation of the eddy. This interpretation is consistent with our results, which show that when an anticyclonic eddy impinges on the Kuroshio near its origin (close to the bifurcation latitude of the NEC), strong lateral streamline confluence causes considerable deformation of the eddy, resulting in the observed narrow, meridionally elongated positive

ridge in the SSHA maps (Figure 7i,j). The acceleration of northward flow driven by interaction between anticyclonic eddies and the Kuroshio further contributes to the offshore velocity core observed downstream (east of Taiwan).

SUMMARY

Nine cross-section Seaglider surveys during 2011–2013 reveal three dual velocity maxima events in the Kuroshio east of Taiwan. This study also investigates potential mechanisms for generating the dual-core Kuroshio structure

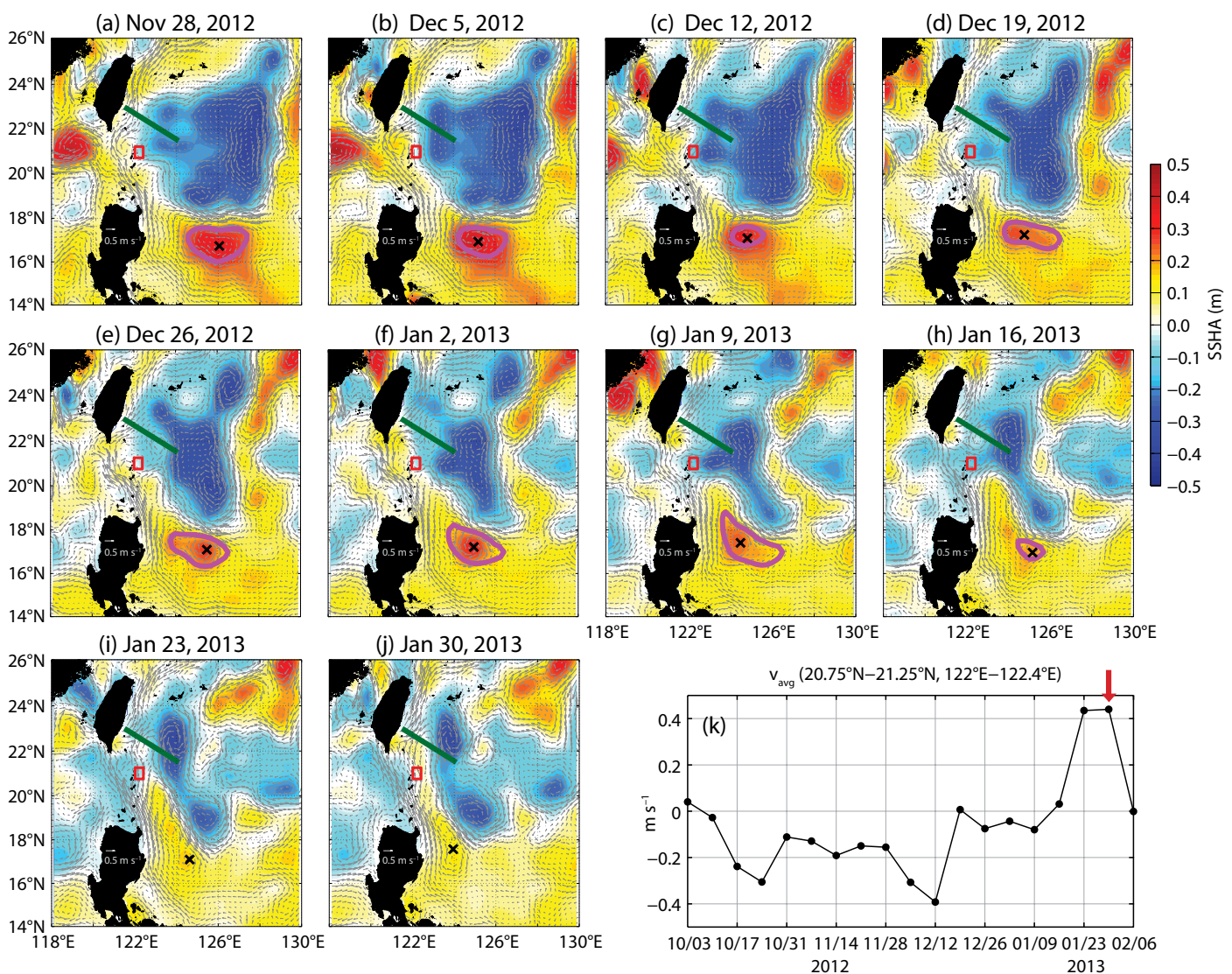



FIGURE 7. (a–j) AVISO SSHA (color shading) and corresponding geostrophic current from November 28, 2012, to January 30, 2013. The green solid line indicates the Seaglider transect along N1. The center position of an anticyclonic eddy is marked by black "x". The boundary of the eddy, defined following Lien et al. (2014), is plotted in magenta. The red box denotes the region of spatial averaging of meridional velocity used for panel (k). (k) Time series of spatially averaged meridional components of AVISO geostrophic current velocity east of Luzon Strait ($20^{\circ}45'N$ – $21^{\circ}5'N$, $122^{\circ}E$ – $122^{\circ}24'E$). The red arrow points to the time when the dual-core event was observed during Survey 8.

east of Taiwan. The Kuroshio's westward intrusion in Luzon Strait occurs preferentially during the northeast monsoon. An intrusion event causes streamline diffuence across the strait. The associated weakening of the Kuroshio's inshore branch, in Luzon Strait, makes the northward flow east of the strait (the offshore branch) become more distinct. Additionally, the quasi-permanent anticyclonic recirculation southeast of Taiwan, which strengthens northward flow in the Kuroshio's offshore side, shifts northward during wintertime. The joint effect of the Kuroshio intrusion, the northward flow east of Luzon Strait, and the recirculation's northward shift drives the streamline confluence zone downstream, leading to more frequent occurrences of the dual-core structure east of Taiwan. This mechanism is most active during the northeast monsoon, and may explain the more frequent presence of the dual-core Kuroshio during this period.

Interactions between the Kuroshio and impinging anticyclonic eddies in the upstream region, for example, east of Luzon Island, also result in the dual-core structure east of Taiwan. The deformation and dissipation of impinging anticyclonic eddies along the east flank of the Kuroshio strengthen the offshore branch of the current east of Luzon Strait, making the offshore core more distinct relative to the inshore core, which flows across Luzon Strait without acceleration.

Glider-observed water masses associated with the two velocity maxima provide evidence consistent with both of these explanations for the formation of the dual-core structure. In cases associated with the Kuroshio intrusion, θ - S properties suggest that the inshore core is primarily SCS waters and the offshore core is WPS waters. In the cases associated with the interaction between the Kuroshio and the westward-propagating anticyclonic eddy in the upstream region, waters in both velocity cores mostly originate from the WPS. 

REFERENCES

- Centurioni, L.R., P.P. Niller, and D.K. Lee. 2004. Observations of inflow of Philippine Sea surface water into the South China Sea through the Luzon Strait. *Journal of Physical Oceanography* 34:113–121, [http://dx.doi.org/10.1175/1520-0485\(2004\)034<0113:OOIOPS>2.0.CO;2](http://dx.doi.org/10.1175/1520-0485(2004)034<0113:OOIOPS>2.0.CO;2).
- Chen, C.T.A. 2005. Tracing tropical and intermediate waters from the South China Sea to the Okinawa Trough and beyond. *Journal of Geophysical Research* 110, C05012, <http://dx.doi.org/10.1029/2004JC002494>.
- Chern, C.-S., S. Jan, and J. Wang. 2010. Numerical study of mean flow patterns in the South China Sea and the Luzon Strait. *Ocean Dynamics* 60:1,047–1,059, <http://dx.doi.org/10.1007/s10236-010-0305-3>.
- Chern, C.-S., and J. Wang. 1998. A numerical study of the summertime flow around the Luzon Strait. *Journal of Oceanography* 54:53–64, <http://dx.doi.org/10.1007/BF02744381>.
- Cushman-Roisin, B. 1994. *Introduction to Geophysical Fluid Dynamics*. Prentice-Hall, New Jersey, 320 pp.
- Ducet, N., P.Y. Le Traon, and G. Reverdin. 2000. Global high-resolution mapping of ocean circulation from TOPEX/Poseidon and ERS-1 and -2. *Journal of Geophysical Research* 105:19,477–19,498, <http://dx.doi.org/10.1029/2000JC900063>.
- Eriksen, C.C., T.J. Osse, R.D. Light, T. Wen, T.W. Lehman, P.L. Sabin, J.W. Ballard, and A.M. Chiodi. 2001. Seaglider: A long-range autonomous underwater vehicle for oceanographic research. *IEEE Journal of Oceanic Engineering* 26:424–436, <http://dx.doi.org/10.1109/48.972073>.
- Farris, A., and M. Wimbush. 1996. Wind-induced Kuroshio intrusion into the South China Sea. *Journal of Oceanography* 52:771–784, <http://dx.doi.org/10.1007/BF02239465>.
- Hsin, Y.-C., C.-R. Wu, and P.-T. Shaw. 2008. Spatial and temporal variations of the Kuroshio east of Taiwan, 1982–2005: A numerical study. *Journal of Geophysical Research* 113, C04002, <http://dx.doi.org/10.1029/2007JC004485>.
- Jan, S., Y.J. Yang, J. Wang, V. Mensah, T.-H. Kuo, M.-D. Chiou, C.-S. Chern, M.-H. Chang, and H. Chien. 2015. Large variability of the Kuroshio at 23.75°N east of Taiwan. *Journal of Geophysical Research* 120:1,825–1,840, <http://dx.doi.org/10.1002/2014JC010614>.
- Kuo, Y.-C., and C.-S. Chern. 2011. Numerical study on the interactions between a mesoscale eddy and a western boundary current. *Journal of Oceanography* 67:263–272, <http://dx.doi.org/10.1007/s10872-011-0026-3>.
- Liang, W.-D., T.Y. Tang, Y.J. Yang, M.T. Ko, and W.-S. Chuang. 2003. Upper-ocean currents around Taiwan. *Deep Sea Research Part I* 50:1,085–1,105, [http://dx.doi.org/10.1016/S0967-0645\(03\)00011-0](http://dx.doi.org/10.1016/S0967-0645(03)00011-0).
- Lien, R.-C., B. Ma, Y.-H. Cheng, C.-R. Ho, B. Qiu, C.M. Lee, and M.-H. Chang. 2014. Modulation of Kuroshio transport by mesoscale eddies at the Luzon Strait entrance. *Journal of Geophysical Research* 119:2,129–2,142, <http://dx.doi.org/10.1002/2013JC009548>.
- Lien, R.-C., B. Ma, C.M. Lee, T.B. Sanford, V. Mensah, L.R. Centurioni, B.D. Cornuelle, G. Gopalakrishnan, A.L. Gordon, M.-H. Chang, and others. 2015. The Kuroshio and Luzon Undercurrent east of Luzon Island. *Oceanography* 28(4):54–63, <http://dx.doi.org/10.5670/oceanog.2015.81>.
- Mensah, V., S. Jan, M.-D. Chiou, T.-H. Kuo, and R.-C. Lien. 2014. Evolution of the Kuroshio tropical water from the Luzon Strait to the east of Taiwan. *Deep Sea Research Part I* 86:68–81, <http://dx.doi.org/10.1016/j.dsr.2014.01.005>.
- Metzger, E.J., and H.E. Hurlburt. 2001. The non-deterministic nature of Kuroshio penetration and eddy shedding in the South China Sea. *Journal of Physical Oceanography* 31:1,712–1,732, [http://dx.doi.org/10.1175/1520-0485\(2001\)031<1712:TNNOKP>2.0.CO;2](http://dx.doi.org/10.1175/1520-0485(2001)031<1712:TNNOKP>2.0.CO;2).
- Nitani, H. 1972. Beginning of the Kuroshio. Pp. 129–163 in *Kuroshio, Its Physical Aspects*. H. Stommel and K. Yoshida, eds, University of Tokyo Press, Tokyo.
- Pickard, G.L., and W.J. Emery. 1993. *Descriptive Physical Oceanography: An Introduction*, 5th ed. Pergamon Press, 320 pp.
- Rudnick, D.L., S. Jan, L. Centurioni, C.M. Lee, R.-C. Lien, J. Wang, D.-K. Lee, R.-S. Tseng, Y.Y. Kim, and C.-S. Chern. 2011. Seasonal and mesoscale variability of the Kuroshio near its origin. *Oceanography* 24(4):52–63, <http://dx.doi.org/10.5670/oceanog.2011.94>.
- Saucier, W.J. 1955. *Principles of Meteorological Analysis*. University of Chicago Press, 438 pp.
- Yuan, D., W. Han, and D. Hu. 2006. Surface Kuroshio path in the Luzon Strait area derived from satellite remote sensing data. *Journal of Geophysical Research* 111, C11007, <http://dx.doi.org/10.1029/2005JC003412>.

ACKNOWLEDGMENTS

This work is supported by grants from the Ministry of Science and Technology of the Republic of China (Taiwan), MOST-103-2611-M-002-011, and the US Office of Naval Research, N00014-10-1-0308 (Lee) and N00014-10-1-0397 (Lien and Ma). The success of the Seaglider operations is largely due to the dedication and commitment of the Integrative Observational Platforms group at the Applied Physics Laboratory, University of Washington. We thank W.-H. Her, W.-H. Lee, S.-C. Shie, B. Wang, and V. Mensah from National Taiwan University, and the captains and crew members of R/Vs *Ocean Researcher I, II, III, and V*, and R/V *Roger Revelle* for their assistance with the fieldwork. The altimeter products used in this analysis were produced by Ssalto/Duacs and distributed by AVISO, with support from CNES (<http://www.aviso.oceanobs.com/duacs>).

AUTHORS

Kai-Chieh Yang (kcyang.apl@gmail.com) is a PhD candidate at the Institute of Oceanography, National Taiwan University, Taipei, Taiwan. **Joe Wang** is Professor, Institute of Oceanography, National Taiwan University, Taipei, Taiwan. **Craig M. Lee** is Senior Principal Oceanographer and Associate Professor, Applied Physics Laboratory, University of Washington, Seattle, WA, USA. **Barry Ma** is Senior Oceanographer, Applied Physics Laboratory, University of Washington, Seattle, WA, USA. **Ren-Chieh Lien** is Senior Principal Oceanographer, Applied Physics Laboratory, University of Washington, Seattle, WA, USA. **Sen Jan** is Professor, Institute of Oceanography, National Taiwan University, Taipei, Taiwan. **Ying Jang Yang** is Associate Professor, Institute of Oceanography, National Taiwan University, Taipei, Taiwan. **Ming-Huei Chang** is Assistant Professor, Institute of Oceanography, National Taiwan University, Taipei, Taiwan.

ARTICLE CITATION

Yang, K.-C., J. Wang, C.M. Lee, B. Ma, R.-C. Lien, S. Jan, Y.J. Yang, and M.-H. Chang. 2015. Two mechanisms cause dual velocity maxima in the Kuroshio east of Taiwan. *Oceanography* 28(4):64–73, <http://dx.doi.org/10.5670/oceanog.2015.82>.